Thin Sample Alloy Solidification in Electromagnetic Driven Convection

A. Kao[1], N. Shevchenko[2], O. Roshchupinka[2], S. Eckert[2], Koulis Pericleous[1]

[1]Centre of Numerical Modelling and Process Analysis, University of Greenwich, London SE10 9LS, United Kingdom
[2]Helmholtz-Zentrum Dresden-Rossendorf, Institue of Fluid Dynamics, P.O. Box 510119, 01314 Dresden, Germany

Corresponding author: a.kao@gre.ac.uk

Abstract

During the directional solidification of Ga-In25%wt., density variations in the liquid cause plumes of solute to be ejected from the interface through natural convection. This can lead to the formation of chimneys during solidification and ultimately freckles. The application of external magnetic fields can be used to suppress these plumes. Two magnetic systems are considered. The first is a rotating magnetic wheel, which provides conditions analogous to forced convection at the solidification interface. The forced convection causes preferential growth of secondary branches and causes the plumes to be transported downstream and back into the bulk. The second is through the application of a static magnetic field that interacts with inherent thermoelectric currents, generating a Lorentz force that drives fluid flow within the inter-dendritic region. However, in the bulk where there are no thermoelectric currents, electromagnetic damping dominates and plumes are stunted. Using a fully coupled transient numerical model each of these systems has been analysed. Comparisons to experiments are given for the cases of natural and forced convection. The experimental setup uses a Hele-Shaw cell with an electric heater and Peltier cooler, allowing for control over the thermal gradient and cooling rate.

Key words: Gallium Indium; Thin Sample Solidification; Natural convection; Forced convection;Thermoelectricmagnetohydrodynamics

Introduction

Convective transport of solute is known to have a dramatic effect on the evolution of the underlying microstructure of alloys during solidification. In many cases the fluid flow is an inherent part of the process, for example, natural convection is significant in alloys that have relatively large density differences between the various components causing plumes of solute to be ejected back into the melt. These can lead to preferential flow channels (or chimneys) and ultimately the formation of freckles. This phenomenon is common in Nickel based super alloys which are widely used in the manufacturing of gas turbine blades [1-3]. Performing direct in situ experimental studies on Nickel based super alloys is very difficult due to the high solidification temperature. An alternative system to study the underlying mechanism is the Gallium-Indium system, which is liquid at room temperature and easy to handle. Furthermore, due to a relatively large density difference between Gallium and Indium, the system exhibits similar flow behaviour to Nickel based super alloys. An *in situ* radiographic technique for Ga-In systems isused in this work to validate the numerical studies. This technique has previously been used by Eckert and co-workers [4-6].

Numerical models have been used to investigate the formation of freckles in castings [7-9], however they have primarily focused on the effects of natural convection flow. This work focuses on the introduction of external forces in the liquid to controlthe fluid dynamics. In the first instance the application of a magnetic wheel generates an alternating magnetic field providing conditions analogous to forced convection close to the solidification front. The secondexperimentconcernsthe application of a static external magnetic field, leading to two effects;the first is electromagnetic damping, the second *thermoelectric magnetohydrodynamics* (TEMHD). The latter is caused by the magnetic flux interaction with thermoelectric currents,localised to the solidification front giving a resultant Lorentz force, hence driving fluid flow. In this work a fully coupled transient 3-dimensional numerical model was applied to each of these cases. The model uses an Enthalpy based method originating from the work ofVoller [10]. This has been substantially extended by Kao et al. [11,12] into a 3-dimensionalmulti-scale method, that includes fluid flow and electromagnetics. The capability to predict the outcome of microstructural modifications due to externally applied forces will allow for macroscopic material properties to be tailored by selective design of these forces.

Governing Equations

Due to the low Reynolds number encountered on the scale of microstructures and thin sample experiments, a simplified form of the incompressibleNavier-Stokes equation is used, representing Stokes flow:

$$\rho \, \frac{d\mathbf{u}}{dt} = -\nabla p + \mu \nabla^2 \mathbf{u} + \mathbf{F} \tag{1}$$

where ρ is the density, $\mathbf{u}$ the velocity, p the pressure, μ the dynamic viscosity and $\mathbf{F}$ is the sum of all the body forces. For natural convection, the body force $\mathbf{F}$ in (1) is given by

$$\mathbf{F}_{NC} = \rho \mathbf{g} f \beta \left(C - C_0 \right) \tag{2}$$

where β is the compositional expansion coefficient, $\mathbf{g}$ is the gravitational acceleration, f is the liquid fraction, C the concentration of solute and C_0 the bulk concentration. In the case of forced convection, $\mathbf{F}_{FC}$ is assumed to be a constant body force acting over the entire domain. Furthermore, due to the relatively small thickness, W of thin samples and low Reynolds number the flow between the plates can be assumed to be Poiseuille flow. By selecting a characteristic bulk mean velocity $\overline{\mathbf{u}}$ the body force can be calculated from

$$\mathbf{F}_{FC} = \frac{\mu \overline{\mathbf{u}}}{2W^2} . \tag{3}$$

For TEMHD, the current density, $\mathbf{J}$ is given by a generalised form of Ohm's law including an extra term accounting for thermoelectric currents [16]

$$\frac{\mathbf{J}}{\sigma} = \mathbf{E} - S\nabla T + \mathbf{u} \times \mathbf{B} \tag{4}$$

where σ is the electrical conductivity, $\mathbf{E}$ the electric field, S the Seebeck coefficient and $\mathbf{B}$ the DC magnetic field. The thermoelectric currents interact with the magnetic field generating a Lorentz force given by

$$\mathbf{F}_{TE} = \mathbf{J} \times \mathbf{B} . \tag{5}$$

In all cases natural convection is present, hence for forced convection $\mathbf{F} = \mathbf{F}_{NC} + \mathbf{F}_{FC}$ and for TEMHD $\mathbf{F} = \mathbf{F}_{NC} + \mathbf{F}_{TE}$.

Problem Description

Solidification of Ga-In25wt%.alloy in a Hele-Shaw cell with dimensions 25 X 35 X 0.15mm^3 was observed by X-ray radiography. The Hele-Shaw cell was cooled at the bottom by a Peltier cooler at a rate of 0.01K/s. An electric heater at the top with variable heating power was applied to maintain a thermal gradient of 1K/mm over the entire cell. A magnetic wheel was applied at the top of the cell to provide forced convection conditions. The sample is cooled from a molten state and at time t = 0s nucleation occurs and solidification of the microstructure propagates from the base of the sample to the top. A schematic of the experimental setup is given in figure 1.
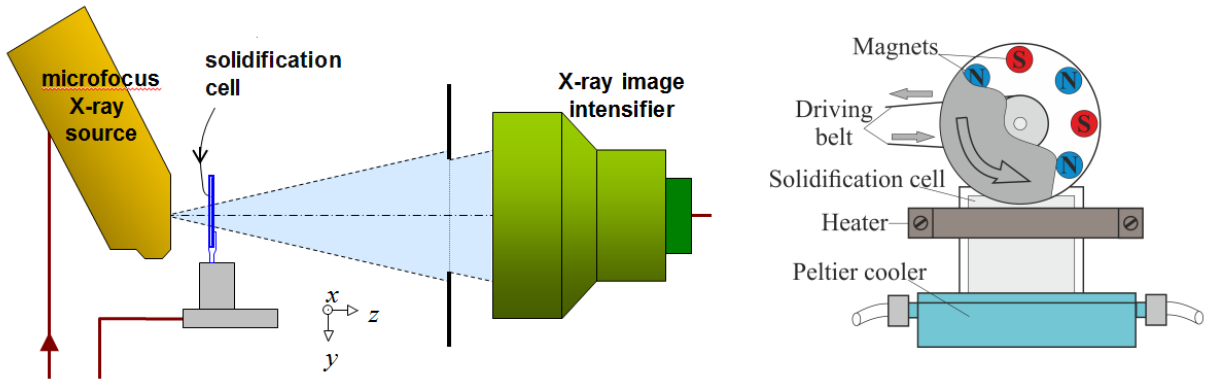

Figure 1.Experimental setup. Left: X-ray radiography system. Right: Hele-Shaw solidification cell with electric heater, Peltier cooler and magnetic wheel.

The numerical model simulates a 5 x 5 x 0.1mm³ region of the solidification cell. The computational grid comprises cubes with a length of 5μm. Table 1 shows the material properties used in the simulation. Periodic boundary conditions are applied on the *x* faces normal to the thermal gradient representing an infinitely wide sample.

Table 1. Material properties used in the numerical model

c_p	2.38×10^6	J/m³/K		ρ	6250	Kg/m³
L	4.2×10^8	J/m³		μ	1.25×10^{-3}	Pas
k	0.5	-		β	1.66×10^{-3}	Wt%$^{-1}$
m	1.8	K/wt%		S	2.5×10^{-7}	V/K
D_l	1.2×10^{-9}	m²/s		σ	3.0×10^6	S/m

Results and discussion

The numerical results for the three test cases are shown in figure 2 in three columns. The top row shows the velocity in μm/s, the bottom row the concentration of Ga in wt%.:

(i)When no magnetic fields are applied, natural convection is the only driver for fluid flow. Plumes of solute are generated by convective rolls close to the interfacethat draw enriched solute from the inter-dendritic region. In most cases, as the inter-dendritic region solidifies and the porosity decreases the convective rolls destabilise and the plumes migrate along the interface.

(ii) The second column shows the effects of the rotating magnetic wheel. Close to the interface the flow is purely by forced convection. Due to the reduction in porosity between the dendrites, the bulk mean flow is significantly larger than any inter-dendritic flow. The flow introduces several significant effects. The first is the preferential growth of secondary arms, which can be attributed to incident bulk concentration flow promoting growth. The second is the increase in primary arm spacing, which is a result of downstream enriched solute being passed from one tip to its neighbour stunting growth. Finally, plumes of solute are transported downstream and back into the bulk.
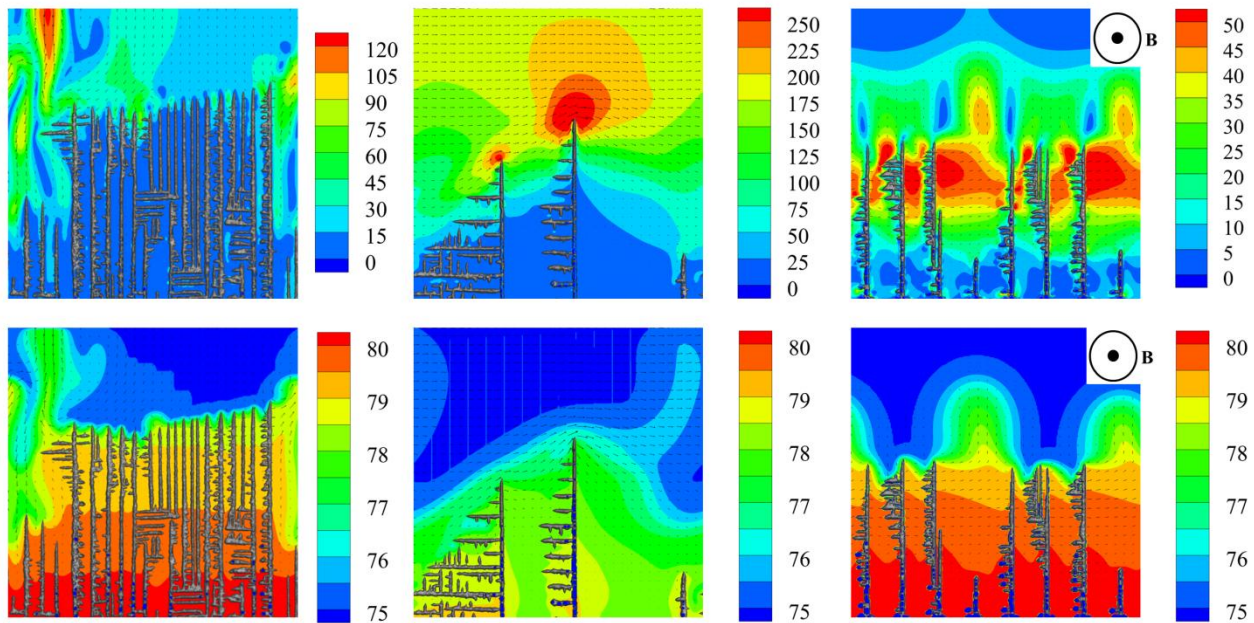

Figure 2.Numerical results showing microstructure morphology, velocity in μm/s (top) and concentration in wt% Ga (bottom) under various magnetic conditions. Left: No magnetic field, natural convection. Centre: Rotating magnetic wheel, forced convection. Right: Static transverse field, TEMHD convection.

(iii) The final case (which at this stage is purely theoretical) looks at TEMHD flow, where relatively high thermoelectric currents exist in the inter-dendritic liquid. Application of a 1T external magnetic field normal to the figure generates a Lorentz force, driving flow in inter-dendritic regions where there is a significant current. However as the porosity decreases the inter-dendritic flow becomes restricted. This creates a region of relatively high velocity that tracks the solidification front. The underlying mechanism is similar to forced convection, as this region of velocity transports

liquid downstream. Depending on the concentration of the liquid, growth is either promoted or stunted. However, in contrast to the case of forced convection, the absence of currents in the bulk combined with electromagnetic damping gives no bulk mean flow. Moreover, electromagnetic damping slows the formation of plumes of solute. The inability to effectively eject solute into the bulk causes the inter-dendritic region to become more enriched compared to the other cases.

Figure 3 shows experimental results with no magnetic field and with forced convection from the rotating magnetic wheel. There is a reasonable agreement of the predicted mechanisms from the numerical analysis and the experimental observations for the two cases tested: The primary arm spacing has increased with convection and secondary arm growth is enhanced against the flow direction. A 'saw tooth' solid front develops due to solute concentration ahead of tall dendrites and plumes of solute are suppressed.
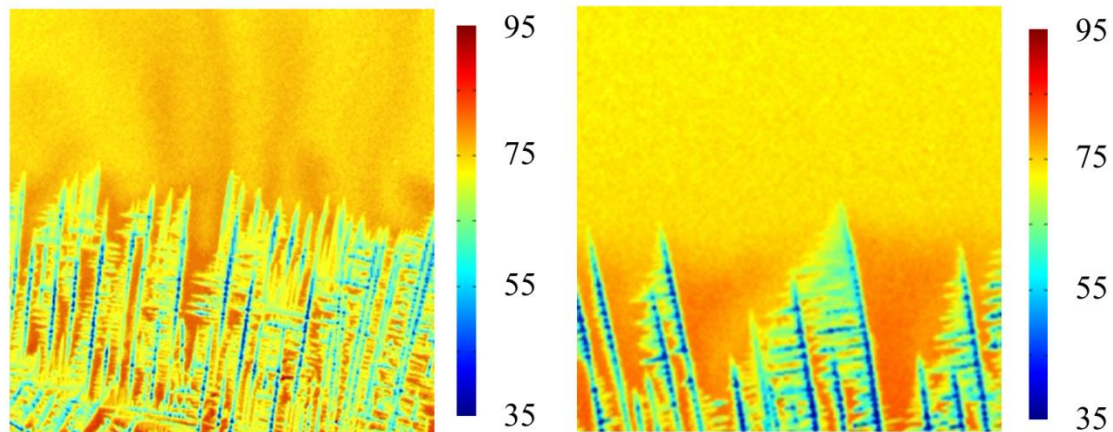

Figure 3.In situ radiographs during solidification of thin sample experiments showing microstructure morphology and concentration (%wt. Ga) in the melt. Left: Natural convection. Right: Forced convection (flow is from left to right).

Conclusions

This work demonstrates the ability to suppress the formation of solute plumes through the use of magnetic fields. The introduction of fluid flow by the magnetic field also changes the microstructure. Through selective design of the magnetic field it is conceivable that the formation of freckles can be prevented allowing for a more reliable method of casting for alloys with large density variations.

References
[1]   Reed R C, Tao T and Warnken N (2009), Acta Mater., 57, pp 5898-5913
[2]   Madison J, Spowart J, Rowenhorst D, Aagesen L K, Thornton K and Pollock T M (2010), Acta Mater., 58, pp 2864-2875
[3]   Beckermann C, Gu J P and Boettinger W J (2000), Metall. and Mater. Trans. A, 31A, pp 2545-2557
[4]   Boden S, Eckert S, Gerbeth G (2010), Mater Lett., 64, pp 1340-1343
[5]   Shevchenko N, Boden S, Gerbeth G and Eckert S (2013), Metall. And Mat. Trans. A, 44, pp 3797-3808
[6]   Boden S, Eckert S, Willers B and Gerbeth G (2008), Metall. Mat. Trans. A, 39, pp 613-623
[7]   Pericleous K A, Djambazov G, Ward M, Yuan L and Lee P D (2013), Metall and Mat Trans A, 44, (12) pp 5365-5376
[8]   Guo, J, and Beckermann, C (2003), Num Heat Transfer, A, 44, pp 559-576
[9]   Karagaddea S, Yuan L, Shevchenko N, Eckert S and Lee P D (2014), Acta Mater., 79, pp 168-180
[10]   Voller V (2007), Int J. Heat Mass Transfer, 51, pp 823-834
[11]   Kao A and Pericleous K (2012), J. Algor. Comp. Tech., (6)1, pp 173-201
[12]   Kao A and Pericleous K (2012), J. of Iron and Steel Research International, (19)1, pp 317-321